AJNR

Lysolecithin-induced demyelination in primates: preliminary in vivo study with MR and magnetization transfer.

V Dousset, B Brochet, A Vital, C Gross, A Benazzouz, A Boullerne, A M Bidabe, A M Gin and J M Caille

AJNR Am J Neuroradiol 1995, 16 (2) 225-231
http://www.ajnr.org/content/16/2/225

Lysolecithin-Induced Demyelination in Primates: Preliminary In Vivo Study with MR and Magnetization Transfer

Vincent Dousset, Bruno Brochet, Anne Vital, Christian Gross, Amid Benazzouz, Anne Boullerne, Anne-Marie Bidabe, Anne-Marie Gin, and Jean-Marie Caille

PURPOSE: To study bystander demyelination in multiple sclerosis with an experimental in vivo model of toxic demyelination. **METHODS:** Toxic demyelinating lesions were created in two monkeys by injection of lysophosphatidylcholine in the centrum semiovale. Follow-up was done clinically and with serial MR studies, including T2-weighted and gadolinium-enhanced T1-weighted images and measurement of magnetization transfer ratio, until the animals were killed at days 14 and 34, respectively. Light and electron microscopy analysis was compared with MR data. **RESULTS:** Interval measurement of magnetization transfer ratio during the course of the experiment revealed a maximum decrease at day 7 to day 8, associated with the greatest clinical manifestations. The lowest values of magnetization transfer ratio correlated with histopathologic findings of myelin and axon destruction. Magnetization transfer ratio measurements appear to be sensitive to macromolecular destruction and specifically to membrane disorganization. At no time was gadolinium enhancement observed in this model of toxic demyelination. **CONCLUSION:** Preliminary results of this study indicated that magnetization transfer is a good technique to follow in vivo matrix destruction in brain parenchyma lesions. The results suggest also that phases of toxic demyelination in multiple sclerosis might not show gadolinium enhancement. Differentiation between demyelinating activity and associated inflammation in multiple sclerosis lesions should be considered in further in vivo work.

Index terms: Magnetic resonance, magnetization transfer; Sclerosis, multiple; Demyelinating disease; Animal studies

AJNR Am J Neuroradiol 16:225–231, February 1995

A variety of histopathologic mechanisms have been implicated in demyelinating disorders such as multiple sclerosis. These include T cell–dependent cytotoxicity, antibody-dependent cytotoxicity, membrane-complement complexes, and toxic factors such as α tumor necrosis factor, nitrite oxide, and lysophosphatidylcholine (LPC) (1–4). To study the various hypotheses concerning the mechanism of demyelination, several animal models have been used. Inflammatory demyelination (acute and chronic experimental allergic encephalomyelitis) has been studied (5, 6). There have been fewer reports concerning in vivo models of toxic demyelination. These experiments have used ethidium bromide and LPC (lysolecithin) (6–13). LPC has been observed to produce focal demyelination followed by remyelination on the rat spinal cord and rabbit corpus callosum. We used magnetic resonance (MR) to study the course of LPC-induced lesions in primates. MR is sensitive to detection of demyelinating diseases. However, it lacks the specificity for distinguishing different pathologic states, especially for differentiating edema from demyelination. The application of magnetization transfer (MT) to study allergic experimental

Received January 19, 1994; accepted after revision June 23.

Supported by grants from INSERM (grant 920907), Pôle GBM, and Laboratoire Guerbet, France.

Presented as a poster exhibit at the World Congress of Neurology Satellite Meeting on Multiple Sclerosis, Victoria, Canada, September 1993.

From the Departments of Neuroradiology (V.D., A.-M.B., A.-M.G., J.M.C.), Neurology (B.B.), Neuropathology (A.V.), Neurophysiology (C.G., A.Benazzouz), and Immunology and Pathology (A.Boullerne), Hospital Pellegrin, University of Bordeaux II, France.

Address reprint requests to Vincent Dousset, MD, Service de Neuroradiologie, Hopital Universitaire Pellegrin, 33076 Bordeaux, France.

AJNR 16:225–231, Feb 1995 0195-6108/95/1602–0225

encephalomyelitis and multiple sclerosis has been reported previously. It was proposed that MT might be able to differentiate edema from myelin destruction (14). MT techniques are sensitive to the surface chemistry of macromolecules and demonstrate a high level of reproducibility (15–17). MT offers the potential to quantify the extent of myelin and axon loss as well as to follow remyelination. Our study is a preliminary attempt to exploit MR techniques, including MT, to monitor the development of lysolecithin-induced demyelinating lesions in an attempt to improve tissue characterization by correlating MT results with histopathologic findings.

Materials and Methods

Two *Macaca fascicularis* adult male monkeys (M1, M2) with respective weights of 5.5 and 6.6 kg were anesthetized using ketamine and xylazine hydrochloride. A solution of L-α-lysophosphatidylcholine stearoyl was slowly injected into the posterior part of the right centrum semiovale via stereotactic craniotomy. The LPC had been diluted previously with sterile serum and guadinine to increase its solubility and diffusion. In animal M1, 150 μl of a 1% LPC concentrated solution was injected over 15 minutes. Animal M2 received 300 μl of a 2% LPC concentration over 30 minutes. A clinical evaluation was achieved every day according to previously published criteria (5).

All MR studies were performed on a 1.5-T superconducting magnet before creation of the lesions and at the following dates: (*a*) for M1, at day 0, 3, 8, 10, 12, 18, 28, and 33; the animal was killed on day 34, after almost complete disappearance of the lesion on the MR images; (*b*) for M2, at day 0, 5, 7, and 12; the animal was killed on day 14, when the lesion had started to decrease in size.

Fig 1. Sagittal locater. Internal landmarks (*arrows*). Anterior landmark, angle between the frontal and sphenoidal bone. Posterior landmark, intersection between the perpendicular internal fissure and the tentorium. Sections were positioned perpendicular to the line between those two landmarks.

Reproducibility of section location on MR studies over the duration of the experiment was insured by using internal landmarks (Fig 1). On the sagittal locater the anterior landmark was the angle between frontal and sphenoidal bone, whereas the posterior landmark was at the intersection between perpendicular internal fissure and the tentorium. Sections were positioned perpendicular to the line between those two landmarks. The posterior aspect of the first section was perpendicular to the occipital cortex. The imaging protocol included a long-repetition-time, long-echo-time, spin-echo T2-weighted sequence 2500/22–90/1 (repetition time/echo time/excitations), as well as an MT protocol. The MT protocol used a two-dimensional gradient-echo sequence (600/10/3) with a 35° flip angle, 128 $\times$ 256 matrix size, 150-mm field of view, 10 4-mm thick sections, and an acquisition time of 4 minutes. This was a reference sequence and was proton density–weighted. This sequence was repeated using the same imaging parameters and the same gain, but an additional off-resonance preparation pulse was used to saturate the macromolecular protons to perform MT contrast. The off-resonance pulse was centered 1500 Hz below the water frequency, with a duration of 16 milliseconds and a bandwidth of 250 Hz.

Those parameters have been evaluated separately to obtain maximum MT effects.

A MT ratio was calculated according to the following equation (15):

$$\text{MT ratio (\%)} = \{1 - [\text{S(MT)}/\text{S(REF)}]\} \times 100,$$

where S(MT) is the signal intensity on the magnetization transfer image and S(REF) is the signal intensity on the reference image.

Signal intensity was calculated from a circular region of interest of 112 pixels, with the mean and standard deviation calculated by Numaris A2.5 software (Siemens, Germany).

Two other sequences were also employed to evaluate blood-brain-barrier disruption. These included a short-repetition-time, short-echo-time, spin-echo T1-weighted sequence pregadolinium (500/22), and a short-repetition-time, short-echo-time, spin-echo T1-weighted sequence postgadolinium.

The animals were killed while under general anesthesia, using the intracardiac perfusion technique with serum and a 2% solution of buffered paraformaldehyde. Electron and light microscopy were performed. After coronal brain cutting, samples for electron microscopy were taken at the sites of abnormal T2 intensity and abnormal MT ratio (ie, at the level of the infusion site [centrum semiovale] on M1 and M2) and from the ipsilateral temporal area on M2. Samples were then fixed in 2.5% glutaral. The two brains were fixed in 10% formalin for 3 weeks and then cut coronally. Hemispheric tissue blocks were embedded in paraffin and sectioned for staining with hematoxylin-eosin, Loyes, and Luxol fast blue.

Fig 2. *A*, Reference image of normal monkey brain (M1 before LPC injection).

B, Image obtained with the same imaging parameters as *A*, in addition to an off-resonance pulse to produce MT effects. Same window and level settings.

Cursors indicate where the MT ratios were calculated: on the site of infusion and on the contralateral site for normal control.

Results

Preliminary MR Studies

The spin-echo images of the monkeys' brains before the experiment were normal. Measurement of the MT ratios in the normal white matter had an average of 49.5% with a standard deviation of 0.6%, which again confirms the high reproducibility of the technique (Fig 2).

Clinical Results

In animal M1 the only detectable symptom was discrete contralateral hemianopsia from day 0 to day 8. The clinical exam then returned to normal until death (day 33).

In animal M2, symptoms were more conspicuous, with increasing left hemiparesia and contralateral hemianopsia from day 0 to day 8. From day 8 to death (day 14), the animal started to recover.

M1 Lesion Results

The development and disappearance of the lesion in animal M1, from day of lysolecithin injection until complete resolution, is displayed in Figure 3. The lesion increased in size until day 8 and then decreased progressively. On MT images the same course was found, with an MT ratio revealing a maximum decrease at day 8 (44.3% versus normal 49%). Figure 4 displays the evolution of the MT ratio on the lesion and normal contralateral site. On the day of death, the MT ratio was still slightly decreased (46.4%); however, the lesion was not seen on T2-weighted or MT images. No gadolinium enhancement was found inside the lesion but was observed along the needle track and slightly on the meninges around the craniotomy.

Pathologic results in animal M1, killed on day 34 (Fig 5), demonstrated minimal pathologic changes, which correlated with the almost complete disappearance of the lesion on MR at day 33. Light microscopy (Fig 5A) revealed a frontoparietal necrotic lesion with vascular hyperplasia, perivascular lymphocytic infiltrates, spongiosis, and microglial proliferation. Another small area of necrosis was present near the ventricle. Electron microscopic examination (Fig 5B) of the specimens from the site of injection showed myelin-axonal lesions and reactive astrocytes. Edema was not identified in any of the pathologic sections.

Fig 3. Spin-echo T2-weighted image of the course of LPC-induced lesion on M1 in the posterior aspect of the centrum semiovale (*arrows* in *A*), day 0 (*A*), day 8 (*B*), day 18 (*C*), and day 33 (*D*). Maximum size was seen at day 8, correlating with maximum clinical symptoms. The lesion was almost invisible at day 33 just before death (day 34).

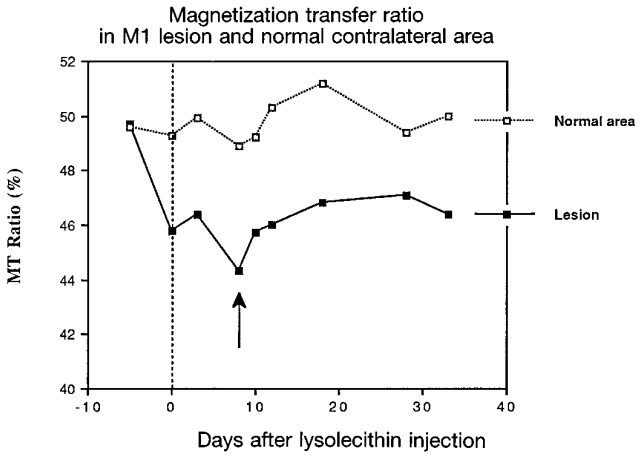

Fig 4. The MT ratio in M1 lesion decreased after the injection, with the lowest value found at day 8 (*arrow*). The MT ratio value tended to return to normal but remained lower than the normal control opposite side even after disappearance of the lesion on MR imaging.

M2 Lesion Results

The development and resolution of the lesion is displayed on Figure 6. The lesion increased dramatically during the first week to a maximum in size around day 7. Mass effect was also noted at that time. At day 12 the lesion started to decrease in size, and there was absence of mass effect. In comparison with the centrum semiovale, the lesion appeared to have higher signal intensity in the temporal lobe. This was especially appreciated on the MT images (Fig 6C). Comparison of the MT ratio in the centrum semiovale and the temporal lobe revealed the maximum MT ratio decrease in both areas was at day 7 (34.3% in the temporal area and 37.7% in the centrum semiovale [Fig 7]). At day 12, MT ratio was still more decreased in the temporal lobe (36.8%) than in the centrum semiovale (44.5%). We focused the electron microscopy on these two areas to correlate MT ratio with pathologic findings. On postgadolinium images, no enhancement was found except along the needle tract.

Pathologic results in animal M2, killed on day 14 (Fig 8), demonstrated: (*a*) on light microscopy (Fig 8A), a large necrotic lesion with vascular hyperplasia and microglial reaction; astrogliosis was observed in the subjacent white matter; (*b*) on electron microscopy (Fig 8B), extensive myelin-axonal lesions, lipid-laden macrophages, and reactive astrocytes; lesions were more extensive in the temporal lobe than in the centrum semiovale, and no edema was found.

Discussion

In demyelinating diseases such as multiple sclerosis, immunologic reactions produce tissue damage (1). Local release of myelinotoxic material at the site of damage may play a fundamental role in increasing the demyelination by a process termed *bystander demyelination*. Several agents have been incriminated in this process including α tumor necrosis factor, nitrite oxide, and LPC (2–4).

Experiments on rats or rabbits using direct injection of LPC, either in the central or peripheral nervous system, demonstrated myelin lysis after a few hours, with maximum electrophysiologic and pathologic changes noted at 1 week (4, 7). LPC is a potent detergent, which at high concentration will solubilize most membranes (18). A gliotic and remyelinating phase producing partial repair of the lesion, together with restoration of conduction, has been identified starting at the second part of the second week (8, 10). In this experiment, the feasibility of a model of toxic demyelination has been tested on only two monkeys, but preliminary results indicated that this model was helpful to study

Fig 5. M1 pathologic sample.

A, Light microscopy, hematoxylin-eosin staining: small area of necrosis (*arrow*) in the area of the needle track (killed at day 34).

B, Electron microscopy: focal myelino-axonal lesion (*arrows*).

Fig 6. *A* and *B*, Spin-echo T2-weighted images of the kinetic of M2 lesion at day 7 and day 12. Image *C* was obtained by MT contrast at day 12. Note that the centrum semiovale (*white arrow*) appears less hyperintense on the MT image (*C*) than on the spin-echo T2-weighted image. The difference of contrast between the centrum semiovale and temporal area (*black arrow*) is greater on the image obtained with MT. MT correlated well with the pathologic analysis, which showed a more extensive destruction in the temporal lobe than in the centrum semiovale.

cerebral matrix destruction with small edema. In addition lesions were extensive, especially on the animal M2, with an extension in the temporal lobe at a distance from the site of injection (centrum semiovale). This may be explained by the diffusing nature of lysolecithin along the white matter fibers (7). Lesions were not only demyelinating but also contained regions of necrosis, found in the vicinity of the needle tract. Axonal losses were also seen distal to the site of injection. Waxman et al reported the same pathologic findings in LPC-induced demyelination in rabbit corpus callosum (7). Discrepancies between lesions in animals M1 and M2 may be explained by the double dose and double concentration of LPC injected in M2, which created a more destructive lesion (18). Nevertheless, our preliminary results may provide information on the possible role of toxic agents incriminated in multiple sclerosis, which may not discriminate between myelin and other membranes and may produce both demyelination and axonal loss.

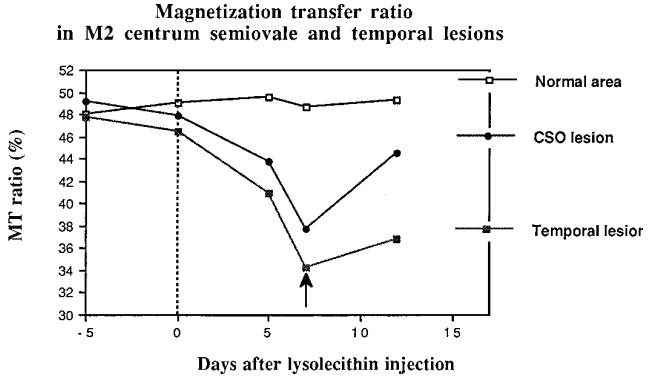

Fig 7. The MT ratio calculated in M2 centrum semiovale and the temporal areas (*cursor* positioned on 6*C*). Maximum decrease was found at day 7 (*arrow*). The temporal lobe had a lower MT ratio. This finding correlated well with the pathologic analysis, which showed a more extensive destruction in the temporal area than in the centrum semiovale (*CSO*).

In our experiment the maximum clinical findings and corresponding largest MR lesions were seen at days 7 to 8. That correlated well with the lowest MT ratios found in both animal lesions at that time. MT is based on the selective interaction between macromolecular and water protons, occurring at the interface between hydrophylic sites of macromolecules and bound water protons (15). Pure water of cerebrospinal fluid does not experience MT, because of absence of macromolecules; neither does subcutaneous or retrobulbar fat, because of the hydrophobic nature of the interactions between water and macromolecules. Normal white matter and gray matter demonstrate high MT effects, probably because of the interactions between hydrophilic sites of membranes (proteins and cholesterol) including myelin membrane, axon and glial cell membrane, and membrane-derived intracellular organs (17). Because of the specific nature of the mechanisms involved in MT, previous study has shown that MT could increase MR specificity for evaluating the amount of tissue damage, specifically myelin loss in demyelinating diseases (14). That was based on in vivo reproducibility of the technique and on comparison with normal MT ratio values in the central nervous system. There were small MT ratio changes in edematous nondemyelinating experimental allergic encephalomyelitis le-

Fig 8. *A*, Light microscopy, hematoxylin-eosin staining: cortical and white matter (*arrows*) involvement of the right hemisphere.

B, Electron microscopy: axon and myelin destruction (*black arrows*), lipid-laden macrophages (*white arrows*).

sions and a wide range of MT ratio values in presumed demyelinated multiple sclerosis lesions in patients. In the present work, heavy demyelinated and necrotic lesions from the monkey killed at almost maximum clinical signs (M2) corresponded to the lowest MT ratio values. The MT ratio appears sensitive to macromolecular destruction and especially to membranes disorganization rather than to edema. Nevertheless, MT ratio does not seem specific to the type of membrane involved. In heavily demyelinated regions with axonal loss, a dramatic drop in the MT ratio values is expected, whereas in less demyelinated lesions, the MT ratio would experience smaller decreases, and only slight changes in the MT ratio are expected with purely edematous lesions. In this experiment, MT ratio values obtained in the lesion site of M1 at the day of death were still slightly low (approximately 4% below normal), but no clinical abnormalities were found, and no abnormal signal was seen on T2 or MT images. MT ratio appeared very sensitive to the minimal histologic changes found in the M1 lesion on light and electron microscopy. That may explain the abnormal MT ratio findings in normal-appearing white matter on both T2 and MT images in multiple sclerosis patients (14). MT technique could be helpful in better understanding the natural history of multiple sclerosis disease.

Gadolinium enhancement was seen only around the needle tract and was caused by local traumatic rupture of the blood-brain barrier and associated inflammatory reaction. No enhancement was seen in the lesions, suggesting that toxic phases of demyelination in multiple sclerosis lesions can occur independent of blood-brain-barrier breakdown (19, 20). Conversely, one can argue that absence of enhancement does not necessarily mean that the blood-brain barrier is intact because of the larger size of the gadolinium chelate compared with water molecules. However, our data support the idea that enhancement in multiple sclerosis lesions may reflect associated inflammatory activity rather than demyelinating activity.

Conclusion

Our preliminary results demonstrate a good correlation between MT and pathologic findings in the differentiation between mild to severe tissue matrix loss in nonedematous toxic demyelinating lesions. Furthermore, absence of gadolinium enhancement in toxic demyelination suggests that enhancement in acute multiple sclerosis lesions may not reflect demyelinating activity of the lesion. This implies that differentiation between inflammatory and demyelinating activities in multiple sclerosis lesions should be considered in further in vivo studies.

Acknowledgments

We thank R. I. Grossman, W. I. McDonald, A. Baron-Van Evercooren, E. C. Alvord and T. Richards for their valuable advice, and Jeannette Richard, Michéle Turmo, and Isabelle Vianes for the quality of their work.

References

1. Compston DAS. Immunological aspects of multiple sclerosis. In: Matthews WB, ed. *McAlpine's Multiple Sclerosis*. 2nd ed. Churchill Livingstone, 1991:321–340
2. Selmaj KW, Raine CS. Tumor necrosis factor mediates myelin and oligodendrocytes damage in vitro. *Ann Neurol* 1988;23:339–346
3. Sherman MP, Griscavage JM, Ignarro LJ. Nitric oxyde-mediated neuronal injury in multiple sclerosis. *Med Hypotheses* 1992;39: 271–274
4. Sedal L, Jennings KH, Allt G, et al. Influence of fatty acid content of lysophosphatidyl choline on its myelinotoxic properties. *Eur Neurol* 1992;32:4–10

5. Stewart WA, Alvord EC, Hruby S, Hall LD, Paty DW. Magnetic resonance imaging of experimental allergic encephalomyelitis in primates. *Brain* 1991;114:1069–1096
6. Rose LM, Richards TL, Alvord EC. Magnetic resonance imaging and peripheral blood abnormalities in experimental allergic encephalomyelitis. *Biomed Pharmacother* 1989;43:347–353
7. Waxman SG, Kocsis JD, Nitta KC. Lysophosphatidyl choline-induced focal demyelination in the rabbit corpus callosum. *J Neurol Sci* 1979;44:45–53
8. Smith KJ, Blakemore WF, McDonald WI. The restoration of conduction by central remyelination. *Brain* 1981;104:383–404
9. Hall S. The effect of injections of lysophosphatidyl choline into white matter of the adult mouse spinal cord. *J Cell Sci* 1972;10: 535–546
10. Blakemore WF, Eames RA, Smith KJ, McDonald WI. Remyelination in the spinal cord of the cat following intraspinal injections of lysolecithin. *J Neurol Sci* 1977;33:31–43
11. Low PA, Schmelz JD, Yao JK, Dyck PJ, Parthasarathy S, Baumann WJ. Structural specificity in demyelination induced by lysophospholipids. *Biochim Biophys Acta* 1983;754:298–304
12. Blakemore WF. Observations on remyelination in the rabbit spinal cord following demyelination induced by lysolecithin. *Neuropathol Appl Neurobiol* 1978;4:47–59
13. Ford CC, Ceckler TL, Karp J, Herndon RM. Magnetic resonance imaging of experimental demyelinating lesions. *Mag Reson Med* 1990;14:461–481
14. Dousset V, Grossman RI, Ramer KN, et al. Experimental allergic encephalomyelitis and multiple sclerosis: lesion characterization with magnetization transfer imaging. *Radiology* 1992;182: 483–491
15. Wolff SD, Balaban RS. Magnetization transfert contrast (MTC) and tissue water proton relaxation in vivo. *Magn Reson Med* 1989;10: 135–144
16. Eng J, Ceckler TL, Balaban RS. Quantitative H1 magnetization transfer imaging in vivo. *Magn Reson Med* 1991;17:304–314
17. Balaban RS, Ceckler TL. Magnetization transfer contrast in magnetic resonance imaging. *Magn Reson Q* 1992;8:116–137
18. Gregson NA. Lysolipids and membranes damage: lysolecithin and its interaction with myelin. *Biochem Soc Trans* 1989;17: 280–283
19. Miller DH, Rudge P, Johnson G, et al. Serial gadolinium enhanced magnetic resonance imaging in multiple sclerosis. *Brain* 1988; 111:927–939
20. Kermode AG, Thompson AJ, Tofts P, et al. Breakdown of the blood-brain barrier precedes symptoms and other MRI signs of new lesions in multiple sclerosis. *Brain* 1990;113(2):1477–1489

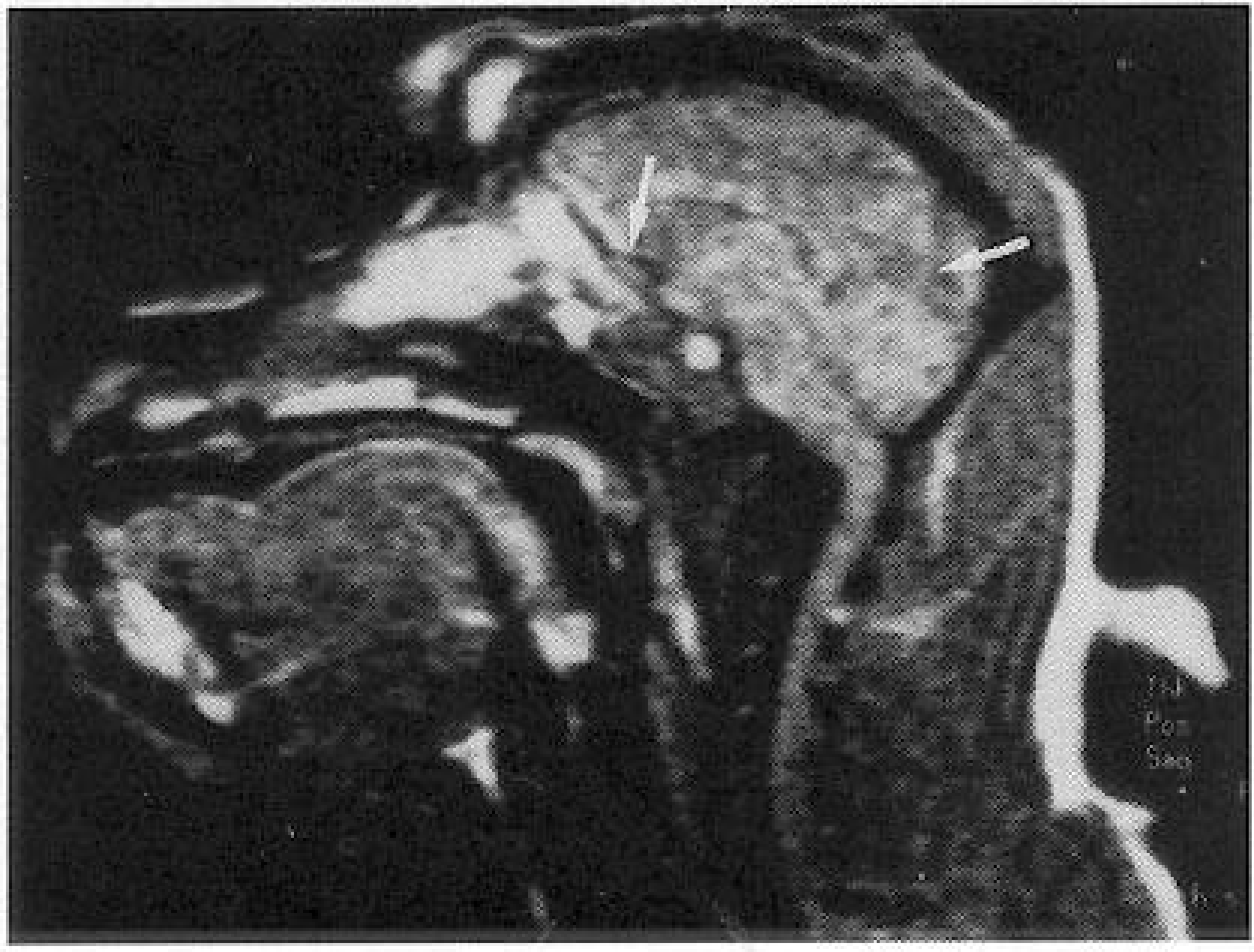

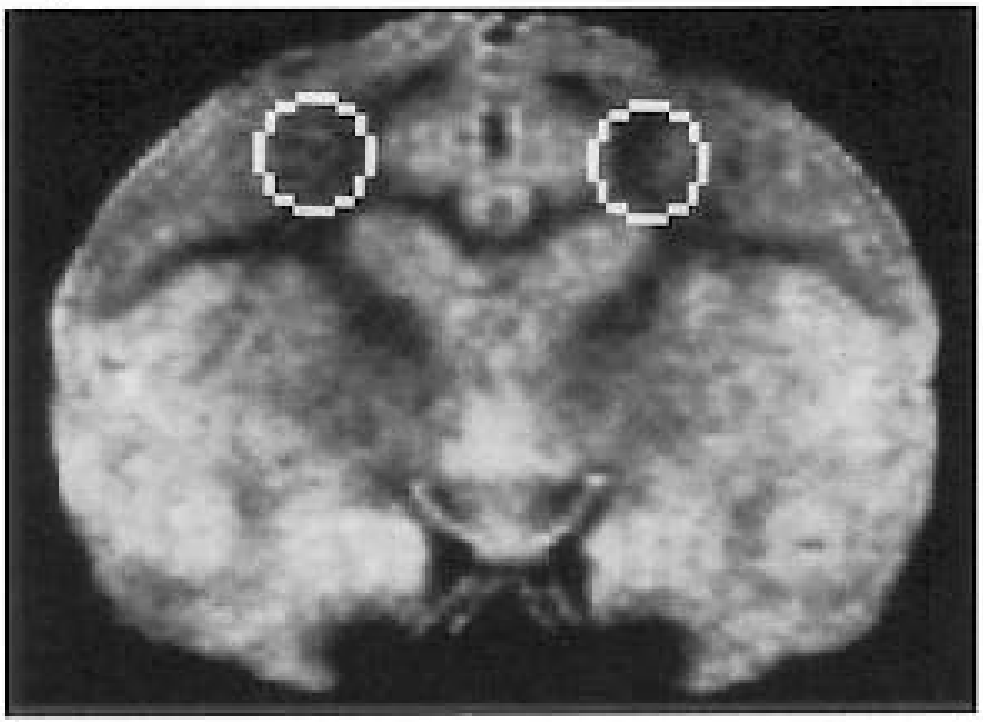

A

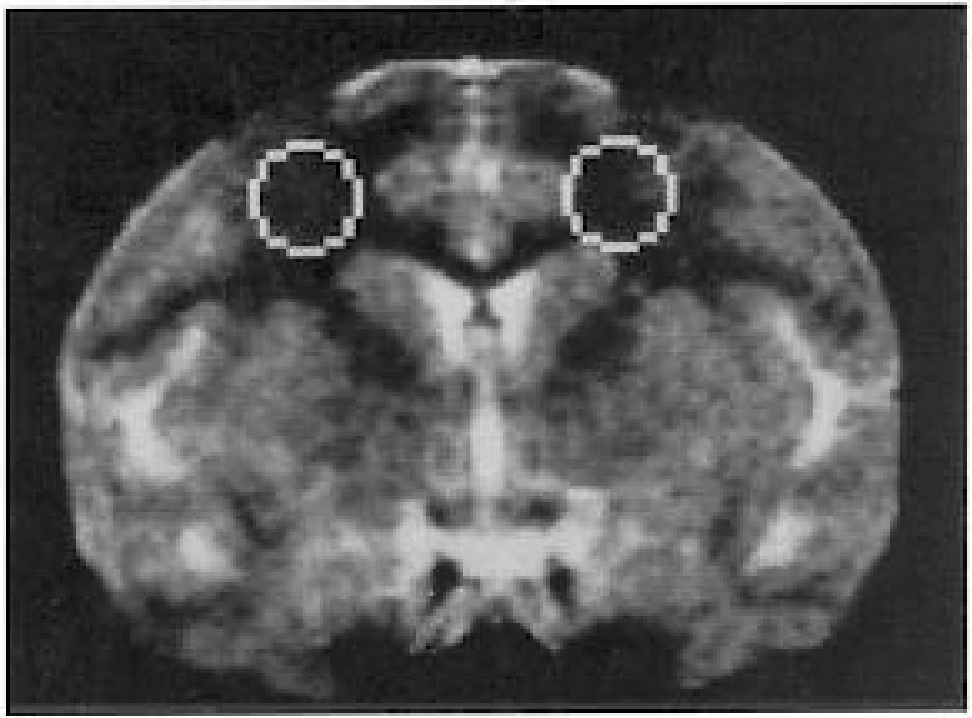

B

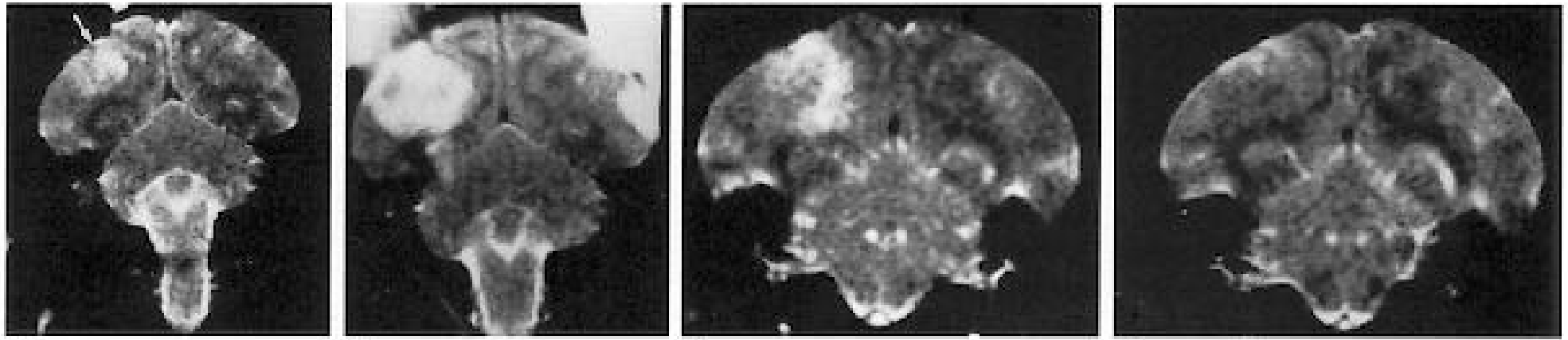
A
B
C
D

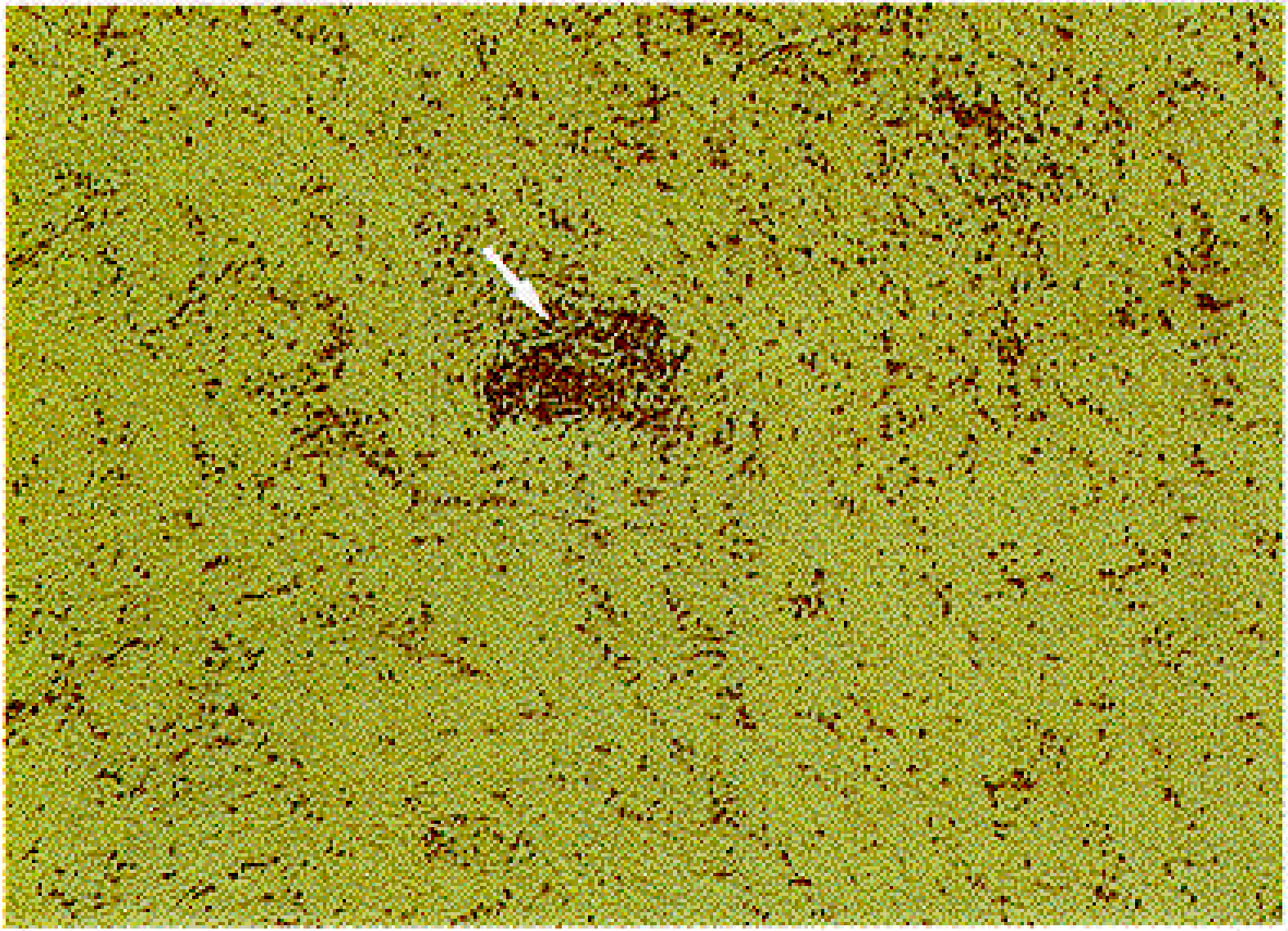

A

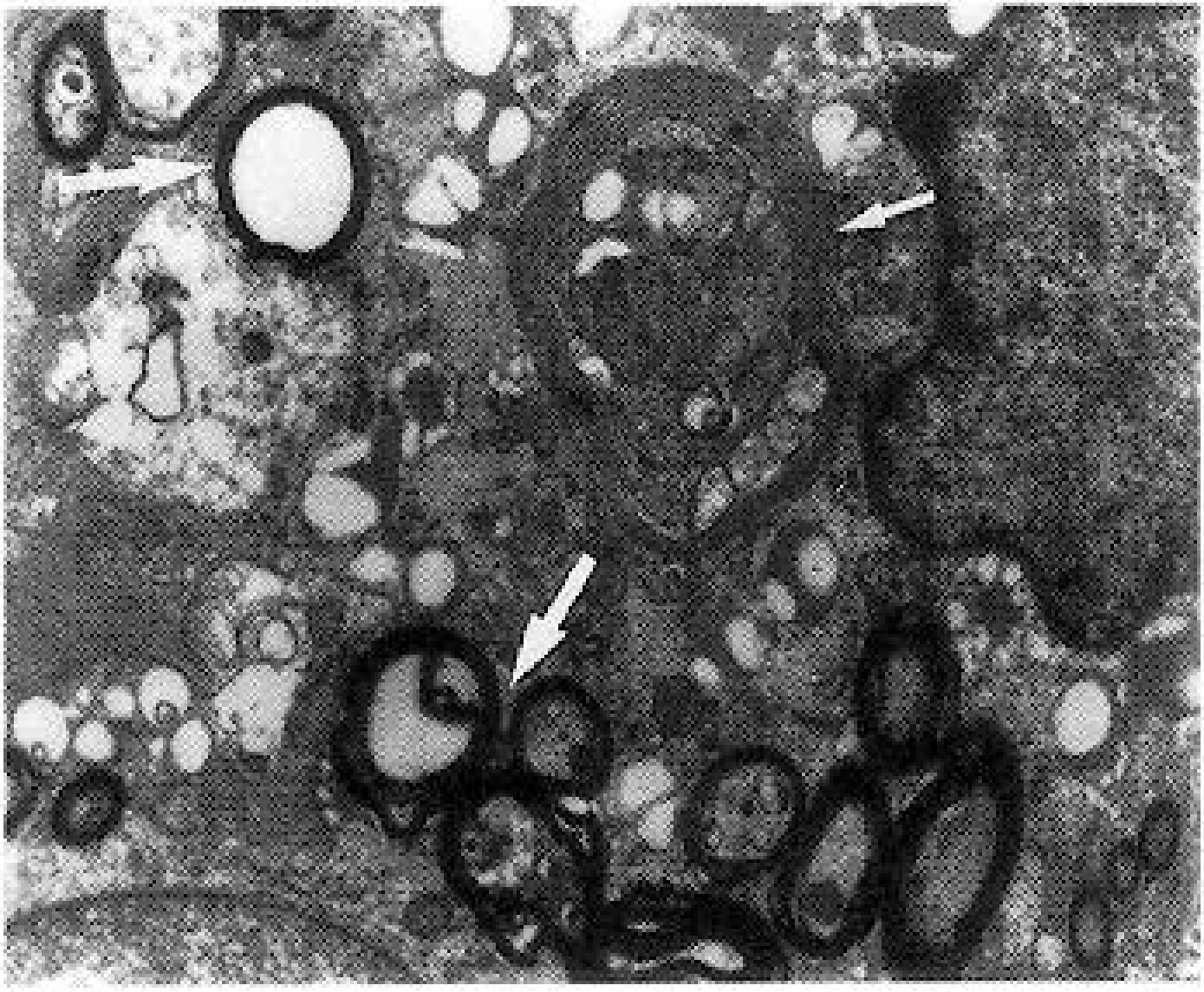

B

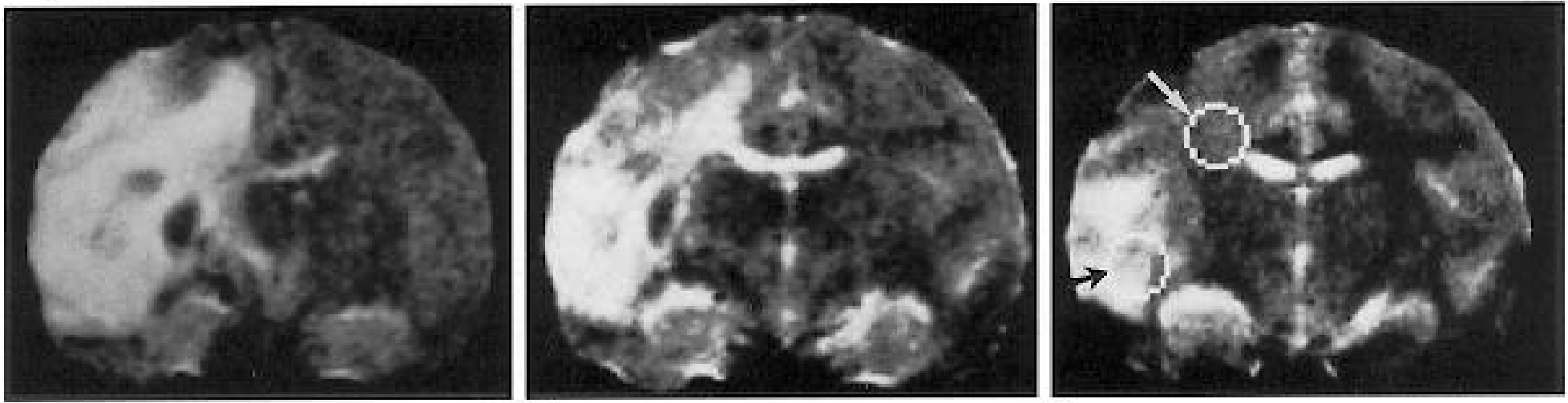
A
B
C

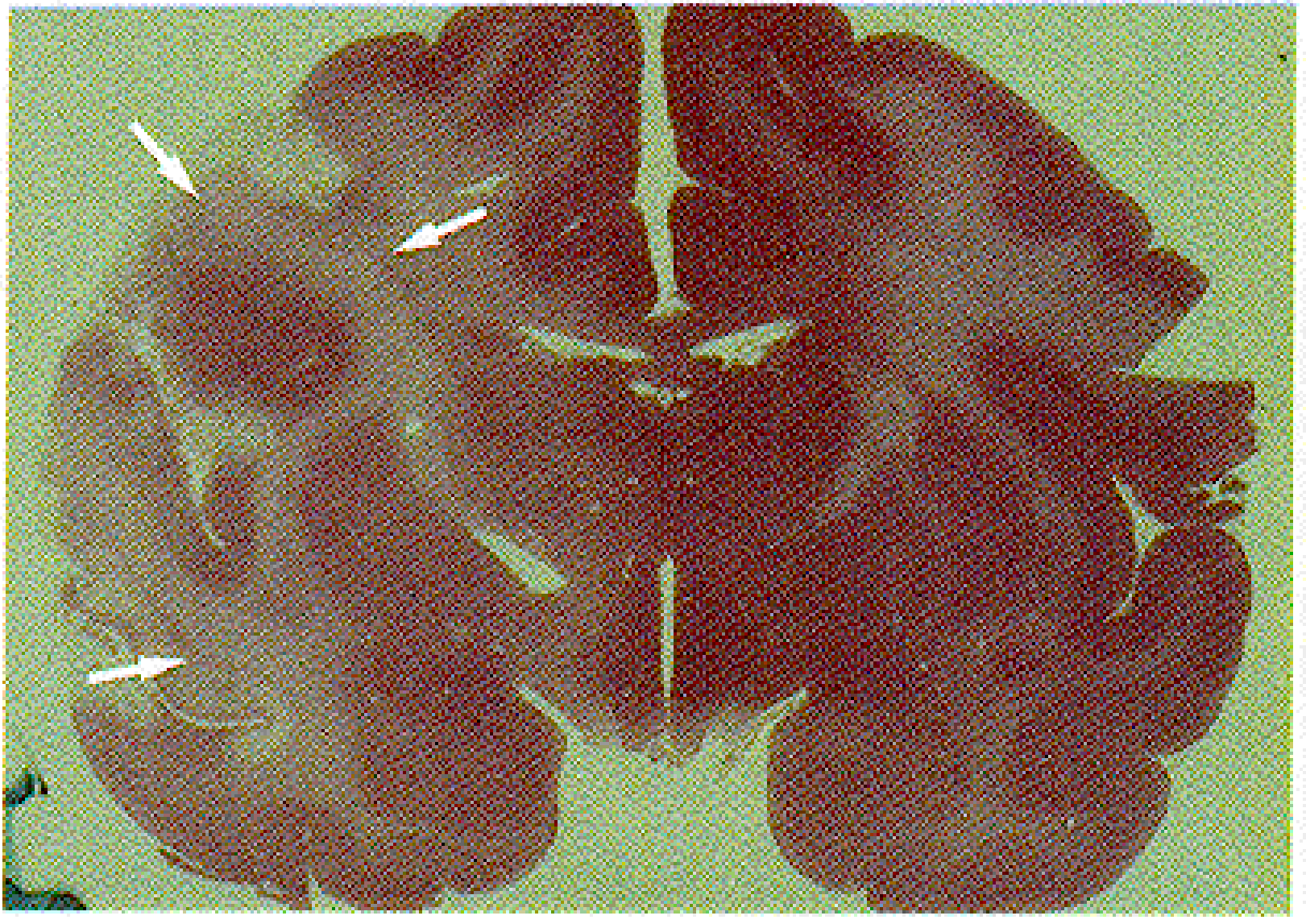

A

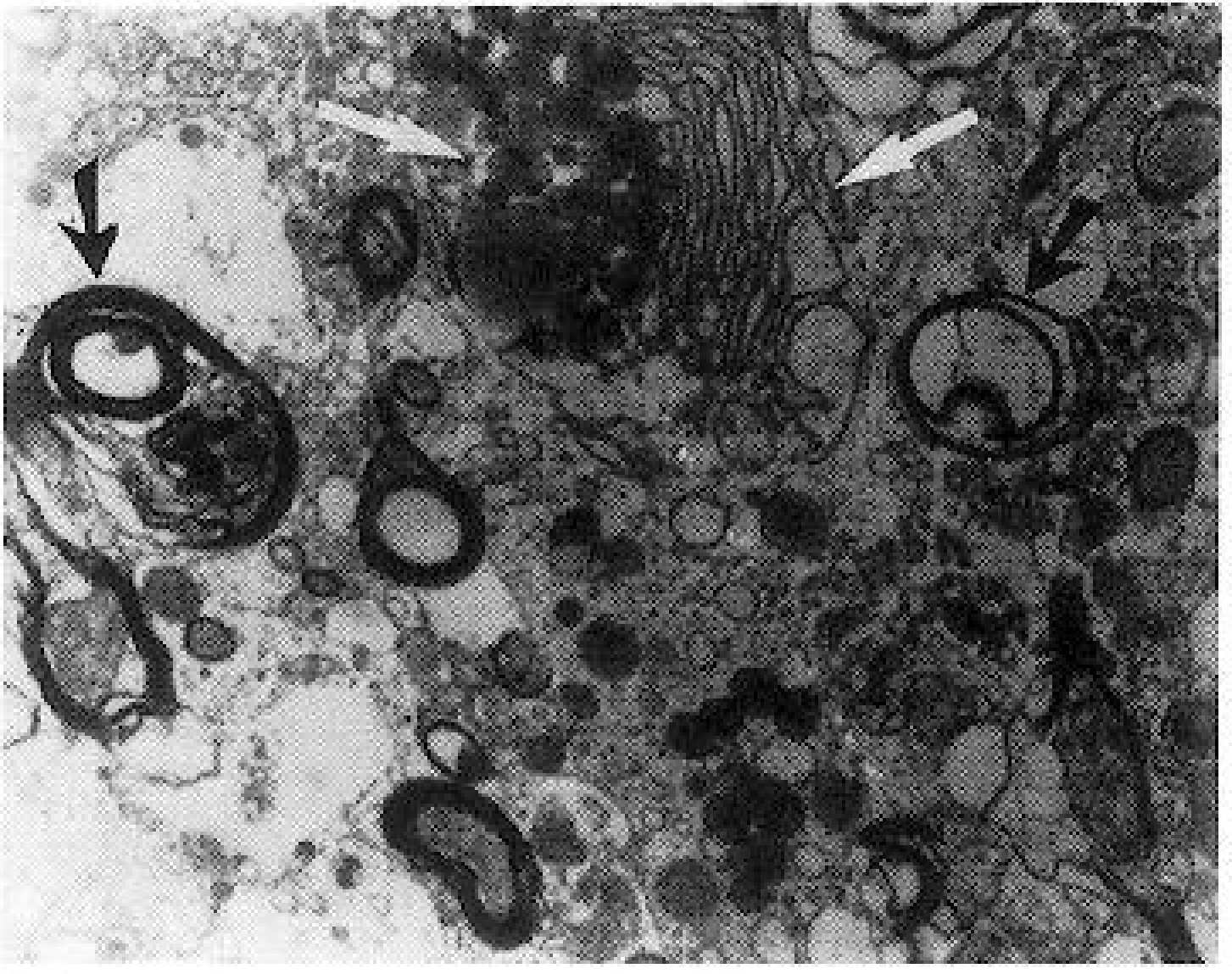

B